BBA - Molecular Basis of Disease 1865 (2019) 1182–1191

Contents lists available at ScienceDirect

BBA - Molecular Basis of Disease

journal homepage: www.elsevier.com/locate/bbadis

Deficiency of perforin and hCNT1, a novel inborn error of pyrimidine metabolism, associated with a rapidly developing lethal phenotype due to multi-organ failure

Sandra Pérez-Torras[a,1], Aida Mata-Ventosa[a,1], Britt Drögemöller[b,c,2], Maja Tarailo-Graovac[d,e,2], Judith Meijer[f], Rutger Meinsma[f], Arno G. van Cruchten[f], Wim Kulik[f], Albert Viel-Oliva[a], Axel Bidon-Chanal[g], Colin J. Ross[b,c], Wyeth W. Wassermann[h], Clara D.M. van Karnebeek[f,h,3], Marçal Pastor-Anglada[a,*,3,4], André B.P. van Kuilenburg[f,**,3,4]

[a] Department of Biochemistry and Molecular Biomedicine, Institute of Biomedicine (IBUB), University of Barcelona, Oncology Program, National Biomedical Research Institute on Liver and Gastrointestinal Diseases (CIBER EHD), Institut de Recerca Sant Joan de Déu (IR SJD), 08028 Barcelona, Spain
[b] Faculty of Pharmaceutical Sciences, University of British Columbia, V6T 1Z3 Vancouver, British Columbia, Canada
[c] BC Children's Hospital Research Institute, V5Z 4H4 Vancouver, British Columbia, Canada
[d] Departments of Biochemistry, Molecular Biology and Medical Genetics, Cumming School of Medicine, University of Calgary, T2N 4N1 Calgary, AB, Canada
[e] Alberta Children's Hospital Research Institute, University of Calgary, T2N 4N1 Calgary, AB, Canada
[f] Departments of Clinical Chemistry, Pediatrics and Clinical Genetics, Amsterdam UMC, University of Amsterdam, Amsterdam Gastroenterology & Metabolism, 1105 AZ Amsterdam, the Netherlands
[g] Departments of Nutrition, Food Science and Gastronomy, School of Pharmacy and Food Science, Institute of Biomedicine (IBUB), Institute of Theoretical and Computational Chemistry (IQTCUB), University of Barcelona, 08921 Santa Coloma de Gramenet, Spain
[h] Departments of Pediatrics and Medical Genetics, Centre for Molecular Medicine and Therapeutics, University of British Columbia, V5Z 4H4 Vancouver, Canada

ARTICLE INFO

Keywords:
hCNT1
Uridine-cytidineuria
Pyrimidine metabolism
PRF1

ABSTRACT

Pyrimidine nucleotides are essential for a vast number of cellular processes and dysregulation of pyrimidine metabolism has been associated with a variety of clinical abnormalities. Inborn errors of pyrimidine metabolism affecting enzymes in the pyrimidine *de novo* and degradation pathway have been identified but no patients have been described with a deficiency in proteins affecting the cellular import of ribonucleosides. In this manuscript, we report the elucidation of the genetic basis of the observed uridine-cytidineuria in a patient presenting with fever, hepatosplenomegaly, persistent lactate acidosis, severely disturbed liver enzymes and ultimately multi-organ failure. Sequence analysis of genes encoding proteins directly involved in the metabolism of uridine and cytidine showed two variants c.1528C > T (p.R510C) and c.1682G > A (p.R561Q) in *SLC28A1*, encoding concentrative nucleotide transporter 1 (hCNT1). Functional analysis showed that these variants affected the three-dimensional structure of hCNT1, altered glycosylation and decreased the half-life of the mutant proteins which resulted in impaired transport activity. Co-transfection of both variants, mimicking the *trans* disposition of c.1528C > T (p.R510C) and c.1682G > A (p.R561Q) in the patient, significantly impaired hCNT1 biological function. Whole genome sequencing identified two pathogenic variants c.50delT; p.(Leu17Argfs*34) and c.853_855del; p.(Lys285del) in the *PRF1* gene, indicating that our patient was also suffering from Familial Hemophagocytic Lymphohistiocytosis type 2. The identification of two co-existing monogenic defects might have resulted in a blended phenotype. Thus, the clinical presentation of isolated hCNT1 deficiency remains to be established.

* Correspondence to: M. Pastor-Anglada, University of Barcelona, Department of Biochemistry and Molecular Biomedicine, 08028 Barcelona, Spain.
** Correspondence to: A.B.P. van Kuilenburg, Amsterdam UMC, Academic Medical Center, Laboratory Genetic Metabolic Diseases, F0-220, Meibergdreef 9, 1105 AZ Amsterdam, the Netherlands.
E-mail addresses: mpastor@ub.edu (M. Pastor-Anglada), a.b.vankuilenburg@amc.uva.nl (A.B.P. van Kuilenburg).
[1] Shared first authors.
[2] Shared second authors.
[3] Co-senior authors.
[4] Co-corresponding authors.

https://doi.org/10.1016/j.bbadis.2019.01.013
Received 17 August 2018; Received in revised form 7 January 2019; Accepted 9 January 2019
Available online 15 January 2019

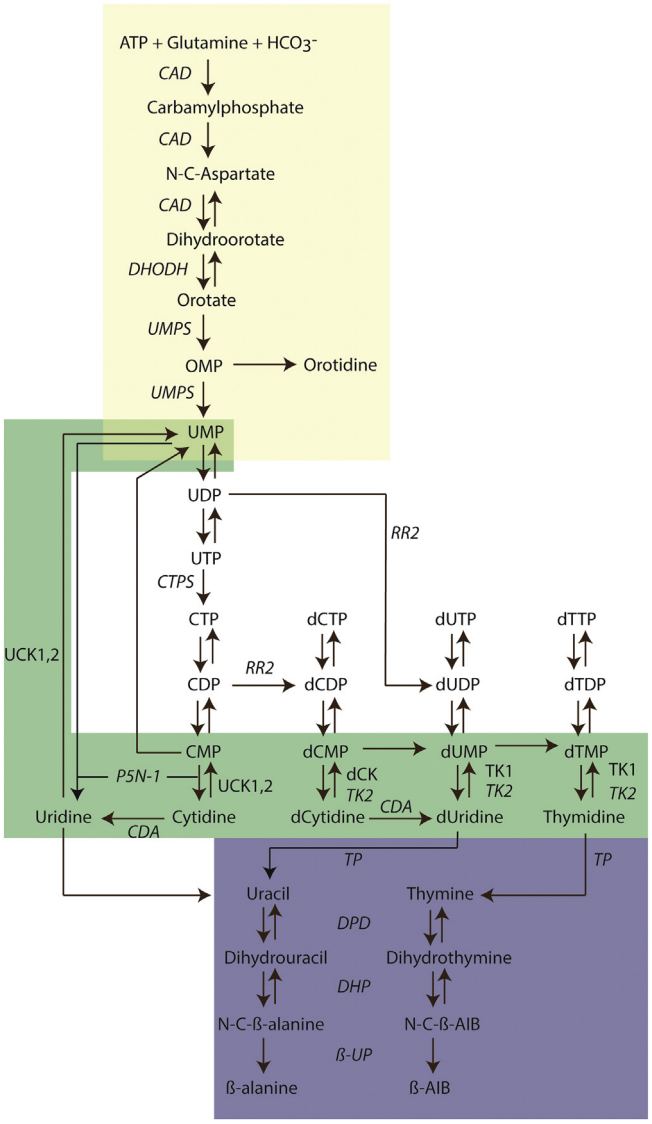

Fig. 1. Schematic representation of pyrimidine metabolism. The pyrimidine *de novo* pathway, salvage pathway and degradation pathway are indicated in yellow, green and purple, respectively. Inborn errors of pyrimidine metabolism are depicted in italics. CAD, Carbamoyl-phosphate synthetase, Aspartate transcarbamylase, Dihydroorotase; CDA, cytidine deaminase; CTPS, CTP synthetase; dCK, deoxycytidine kinase; DPD, dihydropyrimidine dehydrogenase; DHODH, dihydroorotate dehydrogenase; DHP, dihydropyrimidinase; *N*-C-β-alanine, *N*-carbamyl-β-alanine; *N*-C-β-AIB, *N*-carbamyl-β-aminoisobutyric acid; P5N-1, Pyrimidine 5′-nucleotidase type-I; TK1, thymidine kinase 1; TK2, thymidine kinase 2; TP, thymidine phosphorylase; RR2, ribonucleotide reductase; UCK1,2, uridine-cytidine kinase 1,2; UMPS, UMP synthase; β-UP, β-ureidopropionase; β-AIB, β-aminoisobutyrate.

1. Introduction

Pyrimidine nucleotides are essential for a vast number of biological processes such as the synthesis of RNA and DNA. Moreover pyrimidine-activated sugars are also involved in synthesis of phospholipids, glycogen, signal transduction, the sialylation and glycosylation of proteins and lipids and glucuronidation in detoxification processes [1]. In addition, pyrimidines play an important role in the regulation of the central nervous system and metabolic changes affecting the levels of pyrimidines may lead to abnormal neurological activity [2,3].

Pyrimidines can be synthesized *de novo* in mammalian cells through multistep processes (Fig. 1). In addition to the *de novo* synthesis, pyrimidine nucleotides can also be synthesized *via* the salvage of the nucleosides uridine and cytidine. Opposing the action of the enzymes involved in anabolism of pyrimidines are those facilitating the degradation of the pyrimidine nucleosides and pyrimidine bases. The uptake of pyrimidine nucleosides from the extracellular space is mediated by nucleoside-transport proteins that facilitate diffusion or active transport of nucleosides across the plasma membrane. They are encoded by genes belonging to *SLC28* and *SLC29* families [4,5]. *SLC29* genes encode human Equilibrative Nucleoside Transporter (hENT) proteins. This family has four members with only hENT1 (*SLC29A1*) and hENT2 (*SLC29A2*) being plasma membrane nucleoside transporters. The *SLC28* gene family encodes three human Concentrative Nucleoside Transporter (hCNT) proteins, hCNT1, hCNT2, and hCNT3. They all are Na^+-coupled nucleoside transporters showing substrate preference for pyrimidines (hCNT1), purines and uridine (hCNT2), and for both purine and pyrimidine nucleosides (hCNT3).

Genetic defects involving enzymes essential for pyrimidine nucleotide metabolism have provided insights into the vital physiological functions of these molecules [1,3,6]. Inherited disorders of pyrimidine metabolism have a wide variety of clinical presentations which include, among others, anaemia, immunodeficiency, renal stones, convulsions, intellectual disability, autism and growth retardation [6,7]. The majority of the inborn errors of pyrimidine metabolism affect enzymes of the pyrimidine *de novo* synthesis and degradation pathways.

To date, three individuals lacking hENT1 expression have been reported presenting with ectopic mineralization, but *SLC29A1* variants have not been clearly associated with any human disease yet [8]. In contrast, *SLC29A3*, encoding the intracellular transporter hENT3, is the only gene unequivocally linked to several heterogeneous human diseases, such as H syndrome [9], pigmentary hypertrichosis and non-autoimmune insulin-dependent diabetes mellitus syndromes [10], Faisalabad histiocytosis [11] and Rosai-Dorfman disease [11]. A hENT3 deficiency in mouse has been shown to perturb lysosome function, macrophage homeostasis and T-cell performance [12,13]. To date, no patients with pathogenic *SLC28* gene variants have been identified.

The availability of nucleosides and their derivatives are vital for the activation and survival of T-lymphocytes and deficiencies of for example purine nucleoside phosphorylase [14], CTP synthetase 1 [15] and hENT3 [13], resulting in altered nucleoside metabolism, have been shown to compromise immune response. Cytotoxic lymphocytes and natural killer cells eliminate their target cells infected by intracellular pathogens with the help of the cytotoxic pore-forming protein perforin. The perforin pore enables the entry of granzymes into the cytosol of target cells and thus inducing cell death. A deficiency of perforin may result in an impaired ability to handle intracellular infections and malignancies [16].

In this manuscript, we describe the first patient with a combined hCNT1 and perforin deficiency resulting in the onset of a lethal phenotype due to rapid multi-organ failure.

2. Materials and methods

2.1. Reagents and antibodies

Cycloheximide, MG-132, hydroxychloroquine sulfate, tunicamycin, and anti-actin antibody were purchased from Sigma-Aldrich (St. Louis, MO, USA). Anti-CNT1 N17 antibody was obtained from Santa Cruz Biotechnology (Dallas, TE, USA). Dead Receptor 5 (DR5) antibody was purchased from Cell Signaling (Danvers, MA, USA). Microtubule-associated protein 1 light chain 3 (LC3B) was obtained from Cell Signaling. The corresponding horseradish peroxidase (HRP)-conjugated secondary antibodies were obtained from DakoCytomation (Glostrup, Denmark) and BioRad (Hercules, CA, USA).

2.2. Purine and pyrimidine analysis

Concentrations of purine and pyrimidine nucleosides were

determined using reversed-phase HPLC hyphenated with electrospray tandem mass spectrometry [17,18]. Available urine and plasma samples were at a later stage re-analyzed for the presence of cytidine using a MRM for cytidine of 244 > 112, cone voltage 18 V, collision energy 11 eV. The internal standard [^{13}C]-cytidine was analyze using a MRM of 245 > 112.

2.3. Sequence analysis of SCL28A1

Exons 1–18 of *SCL28A1* (hCNT1) and their flanking sequences were amplified using the primer sets, as described in supplementary table 1. Amplification was carried out in 25 μL reaction mixtures containing 20 mM Tris/HCl (pH 8.4), 50 mM KCl, 1.0 mM $MgCl_2$, 0.4 μM of each primer, 0.2 mM dNTPs and 0.02 U of Platinum™ *Taq* polymerase (Invitrogen™). After initial denaturation for 5 min at 95 °C, amplification was carried out for 30 cycles (30 s 95 °C, 30 s 55 °C, 60 s 72 °C) with a final extension step of 10 min at 72 °C. PCR products were separated on 1.5% agarose gels and visualized with ethidium bromide. PCR products where treated with exoSAP-IT and used for direct sequencing. Sequence analysis of genomic fragments amplified by PCR was carried out on an Applied Biosystems model 3730 automated DNA sequencer using the Big dye-terminator method. *SLC28A1* sequence of the patient and controls where compared to reference sequence of *SLC28A1* (Ref Seq NM_001287762.1).

2.4. Whole genome sequencing

Singleton whole genome sequencing (WGS) was performed through the TIDEX gene discovery project (UBC IRB approval H12-00067) using the Illumina HiSeq 4000 (Macrogen, Korea). The sequencing reads were aligned to the human reference genome version hg19 and rare variants in both nuclear and mitochondrial DNA were identified and assessed for their potential to disrupt protein function, and subsequently screened under a series of genetic models: homozygous, hemizygous, compound heterozygous and mitochondrial using our default semi-automated bioinformatics pipeline [19].

2.5. Cell culture and transient transfection

Human Embryonic Kidney 293 cell line (HEK293) was purchased from American Type Culture Collection (ATCC, Promochem Partnership, Manassas, VA, USA) and maintained at 37 °C in a humidified atmosphere containing 5% CO_2, in Dulbecco's modified Eagle's medium (DMEM, Lonza Verviers SPRL, Verviers, Belgium) supplemented with 10% (v/v) fetal bovine serum, 2 mM glutamine, and a mixture of antibiotics (20 U/mL penicillin and 20 μg/mL streptomycin) (Life Technologies, Carlsbad, CA, USA). Cells were subcultured every 3–5 days and confirmed to be mycoplasma free every two weeks by PCR amplification. HEK293 cell line was transiently transfected with the pcDNA3.1-hCNT1 vectors with calcium phosphate.

2.6. Plasmid construction and site-directed mutagenesis

hCNT1 cDNA was cloned from human liver into the expressing vector pcDNA3.1. The R510C and R561Q substitutions were introduced into pcDNA3.1-hCNT1 by Phusion High-Fidelity DNA polymerase (Thermo Scientific, Waltham, MA, USA) using complementary reverse primers, and forward primers containing the variants: R510Cfw 5′-CAAGCAATGCCGCCTGGCAGGGGCCGAG-3′, R510Crv 5′-CTGCCAG GCGGCATTGCTTGTACTTGGAGA-3′, R561Qfw 5′-GGTCCCCCAACAGA AGAGCGACTTCTCC-3′, R561Qrv 5′-CGCTCTTCTGTTGGGGGACCATG GAGGT-3′. The R510C;R561Q was generated introducing the R510C substitution into pcDNA3.1-hCNT1(R561Q) with the same primers. All the constructs were verified by DNA sequencing (BigDye Terminator v3.1, Applied Biosystems, Foster City, CA, USA). Green fluorescent protein (GFP)-fused constructs for each hCNT1 were generated by subcloning each insert to pEGFP-C1 (Clontech, Mountain View, CA) vector. All constructs were used for transient transfection.

2.7. Nucleoside transport assay

Cytidine uptake rate was measured by incubating cell monolayers at room temperature for 1 min with [^{3}H] labeled cytidine (1 μM, 1 μCi/mL; Moravek Inc., Brea California, USA) in a sodium-rich or sodium-free transport buffer (137 mM NaCl or 137 mM choline chloride, 5 mM KCl, 2 mM $CaCl_2$, 1 mM $MgSO_4$, and 10 mM HEPES, pH 7.4). Transport was stopped by washing with cold stop solution (137 mM NaCl and 10 mM HEPES, pH 7.4). Cells were solubilized with 100 mM NaOH containing 0.5% Triton-X100. Protein was determined by BCA reaction (Pierce, Thermo Scientific) and the remaining volume was used for radioactivity counting.

2.8. Western blot analysis

Cell extracts were obtained with lysis buffer (20 mM Tris-HCl pH 8.0, 150 mM NaCl, 10 mM EDTA, 10 mM $Na_4P_2O_7$, 1 mM Na_3VO_4, 100 mM NaF, 1 mM β-glycerophosphate, 1% Igepal CA-630) containing 1% Complete Mini protease inhibitors (Roche, Mannheim, Germany). Protein concentration was determined by Bradford assay (Bio-rad, Hercules, CA, USA). 40 μg of protein of cell lysates were resolved by SDS-polyacrylamide gel electrophoresis on 10% gels, and transferred to polyvinylidene difluoride (PVDF) membranes by standard methods. Membranes were immunoblotted with the indicated primary antibodies. A chemiluminiscence detection kit (Biological Industries, Kibbutz Beit Haemek, Israel) was used to detect antibody labeling.

2.9. Plasma membrane localization of hCNT1

The localization of the different hCNT1 forms was addressed by confocal microscopy. GFP fused proteins were transfected into HEK293 cells cultured on glass coverslips. Glass coverslips were incubated with 1 μg/mL wheat germ agglutinin conjugated to tetramethylrhodamine B isothiocyanate (WGA-TRITC), and with bisBenzimide H 33342 1 μg/mL (Sigma-Aldrich) for 10 min at room temperature. Cells were rinsed three times in phosphate-buffered saline, fixed for 15 min in 4% paraformaldehyde at room temperature, and rinsed three times in phosphate-buffered saline. Glass coverslips were mounted with ProLong Gold antifade reagent (Thermo Scientific). Images were obtained using a laser-scanning confocal microscope (Leica TCS SP2, Leica Microsystems).

2.10. Homology modelling

The model of the hCNT3 transporter was built using the crystal structure of vcCNT (PDB ID: 3TIJ) [20]. MOE (*Molecular Operating Environment* (MOE), 2013.08; Chemical Computing Group ULC, 1010 Sherbooke St. West, Suite #910, Montreal, QC, Canada, H3A 2R7, 2018.) was used to derive a series of homology models upon sequence alignment between the vcCNT crystal structure and the target hCNT3 sequence. The usual protein model verification tests were run to ascertain the correctness of the structure, including the calculation of the overall contact energies, phi-psi angle populations and verification of angle, distance and contact energy properties throughout the structure.

2.11. Supplementary materials and methods

A detailed description of the methodology describing the minigene approach and the investigation of variants identified in the index patient are described in the supplementary data section.

2.12. Statistical analysis

Statistical analysis was performed by multivariant ANOVA testing to compare experimental data of at least three independent experiments with GraphPad Prism software (La Jolla, CA, USA). Significance of multiple comparisons was assessed by post-hoc Tukey test.

3. Results

3.1. Clinical evaluation

The patient is the second-born male child of healthy, non-consanguineous mother (G2P1) and father originating from the Dutch Antilles. The information available for the family history is limited, but largely unremarkable. Pregnancy was complicated by early contractures, possibly related to myomata of the uterus, as well as gradual onset oligohydramnios, which in combination with a breech position, resulted in a planned primary caesarean section at 38 + 1 week. A male was born with a weight of 2750 g, Apgar scores of 9 and 10 after 1 and 5 min respectively; physical exam was unremarkable, including normal size spleen and liver, and tonus. On day 1 he had hypoglycaemias (glucose 2.1 mmol/L at 1 h; 1.9 mmol/L at 6 h) for which glucose infusions were given, with full recovery on day 2.

During the following weeks the mother noticed irritability and 2–3 min episodes of symmetrical jerky limb movements. At 3 weeks he was re-admitted for seizure evaluation and found to be hypertonic. Liver and spleen were not enlarged. Brain sonography, glucose levels, as well as electrolytes and blood gas, were within normal limits. Repeated EEGs showed multifocal theta activity on an immature background, without epileptic activity. The paediatric neurologist concluded the movements to be myoclonia and not epilepsy. At home the spontaneous movements continued. As metabolic evaluation of urine showed increased levels of uridine, he was re-admitted for further clinical evaluation at 2 months of age. Length was 53 cm (80th percentile), weight 4800 g (98th percentile), and occiptofrontal circumference 38.5 cm (90th percentile). He had a mild fever, with an X-thorax showing signs of pneumonia with pleural effusions; intravenous antibiotics were started. Repeated metabolic analysis of urine showed persistently increased uridine excretion.

The fever disappeared with antibiotic management, but the boy became more ill. Haematologic parameters pointed to a viral infection, although all serological parameters have remained negative. He developed a lactate acidosis [pH 7.22 (ref: 7.35–7.45)]:, BE −6.9 mmol/L; (ref: −3 to +3) lactate 16.6 mmol/L (ref: 1.1–3.5), severely abnormal liver enzymes (ASAT 2242 U/L (ref: 9–90); ALAT 678 U/L (ref: 13–45); gammaGT 127 U/L (ref: 8–90); LDH 4695 U/L (ref: 180–430)) and gradual ascites and respiratory insufficiency. Patient was intubated for full respiratory support; lactic acidosis worsened (pH 6.88, BE −24 mmol/L; lactate 17.4 mmol/L) accompanied by hypoglycaemia (glucose 1.9 mmol/L; ref: 2.8–5.5). Abdominal sonography showed a mildly enlarged liver (max diameter 8.0 cm; ref.: 4.7–7.5 cm), a markedly enlarged spleen (diameter 8.0 cm; ref.: 3.0–6.0 cm) and acute necrosis of the renal cortex. Echocardiography showed normal cardiac structure and function, as did sonography of the brain. The patient developed multi-organ failure and died at 9 weeks of age; permission for autopsy was not obtained.

3.2. Pyrimidine nucleosides and variant analysis of SLC28A1

As part of a selective screening program for inborn errors of metabolism, the purine and pyrimidine metabolites were analyzed in urine and plasma. The urine samples showed strongly elevated levels of uridine and cytidine when compared to controls (Table 1). However, normal levels of uridine and slightly elevated levels of cytidine were observed in plasma.

Sequence analysis of genes encoding proteins directly involved in the metabolism of uridine and cytidine was performed and no pathogenic variants were detected in *UPP1*, *UPP2*, *UCK1* and *UCK2* (Supplemental Fig. 1). Sequence analysis of the genomic sequences of exons of *SLC28A1* (Ref Seq NM_ NM_001287762.1), including their flanking intronic sequences, demonstrated the presence of 4 intronic, 4 synonymous, 4 missense variants and an in-frame insertion of 3 nucleotides (Supplemental Table 2). Among these 13 variable sites in *SLC28A1*, two rare variants were observed, including 1 intronic variant (c.97–10C > T) and 1 missense variant c.1682G > A (p.R561Q). The c.1528C > T (p.R510C) variant is relatively infrequent in the European population but particularly common in the East Asian population with a minor allele frequency of 1.6% and 36%, respectively (Supplemental Table 2). The proximity of the c.97–10C > T variant to the splice-acceptor site of exon 3, prompted us to develop a minigene which showed that the c.97–10C > T variant did not affect pre-mRNA splicing (Supplemental Fig. 2).

Table 1
Pyrimidine nucleosides in the patient with a hCNT1 deficiency.

	Patient			Controls (range)[a]
Age	4 weeks	8 weeks	9 weeks	
Urine (mmol/mol creatinine)				
Uridine	102	56	48	0.06–2.5 (n = 50)
Cytidine	n.a.	12.6	5.0	0.08–2.2 (n = 50)
Plasma (μM)				
Uridine	n.a.	4.6	6.5	1.3–9.4 (n = 39)
Cytidine	n.a.	0.6	n.a.	< 0.1–0.2 (n = 39)

n.a., not available.
[a] Age-matched reference range (0–2 years).

Since no gDNA was available from the parents to determine the mode of inheritance of the two missense variants, an allele specific PCR analysis was performed. As rs2242047 (c.1528C > T; p.R510C) and rs149246522 (c.1682G > A; p.R561Q) are 9119 bp apart, smaller allele specific PCRs were performed to determine whether a variant occurring between these variants (rs28430562 A/G) was in *cis* or *trans* with rs2242047 and rs149246522. The whole genome sequencing (WGS) data showed that this variant was heterozygous in the patient. These analyzes confirmed that rs2242047 and rs149246522 occur in *trans* in the patient (Supplemental Fig. 3).

3.3. hCNT1 variants R510C and R561Q may affect tertiary structure

The hCNT1 structure was analyzed to ascertain if the c.1528C > T (p.R510C) and c.1682G > A (p.R561Q) variants could be associated with an impaired function of this transporter, thereby explaining the uridine-cytidineuria of this patient. The impact on hCNT1 protein structure of both p.R510C and p.R561Q was analyzed in a hCNT1 model built up by using homology modelling. The model was generated taking advantage of the resolved crystal structure of the prokaryotic nucleoside concentrative transporter vcCNT [20] as previously published [21]. According to this model, p.R510C is extracellular whereas p.R561Q is facing the cytosol (Fig. 2A). The analysis of both variants showed that these changes individually might induce the loss of interactions involved in the tertiary structure stabilization (Fig. 2B). R510 interacts with the negative charge of ASP503 through a charge-charge interaction and through hydrogen bonds with GLN461 and ASN443. On the other side, R561 has similar interactions with ASP564, LEU330, ALA 331 and MET333. Mutation to cysteine causes a drastic change in the interaction pattern of both residues due to its increased hydrophobic nature and shorter side-chain, presumably affecting the stability of the protein or its capacity to interconvert.

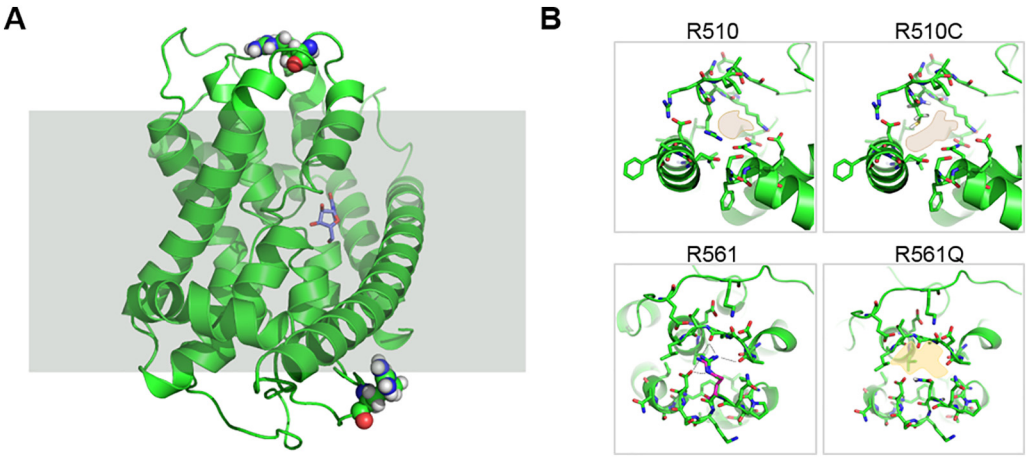

Fig. 2. Changes in the residue interaction pattern upon variant of R510 and R561 of hCNT1. R510 (top, left), R561 (bottom, left) and the residues surrounding them are represented in sticks showing their interactions. The same representation but for the R510C variant is shown on the top right panel. On the bottom left panel, representation in sticks of the R561Q variant and the residues surrounding it. Both variants generate changes in the residue interaction pattern and the residue occupied volume.

3.4. hCNT1 variants impair transport activity

To determine the functional effect of these variants, the wild type (WT), both individually mutated p.R510C and p.R561Q, and the double mutated (p.R510C;p.R561Q) constructs were generated and transfected into human embryonic kidney 293 (HEK293) cells. HEK293 cells were chosen as background for heterologous expression of this transporter protein because they lack hCNT1 activity [21]. The double-mutated hCNT1 was engineered for informative purposes to unveil the functional impact of both variants on transporter expression and performance but might not have clinical relevance because the patient was compound heterozygote for each individual variant. Transport activity of [^{3}H]cytidine of the two variants individually was significantly reduced after 24 h of transfection (Fig. 3A), although with less differences at 48 h (Fig. 3B). Meanwhile, however, the double mutant exhibited a dramatic decrease in activity at both time points (Fig. 3). Moreover, the expression patterns of the three transporters were different from the WT, especially regarding the higher molecular weight bands, which appeared to be directly related to the transport activity (Fig. 3). Thus, the upper bands increased at 48 h for p.R510C and p.R561Q, whereas for p.R510C;p.R561Q the upper bands were undetectable at both time points assayed.

The same three constructs fused at the N-terminal to GFP were transfected with the plasma membrane marker WGA-TRITC to determine their localization. In line with the previous results, p.R510C and p.R561Q were predominantly located at the cell membrane, mainly at 48 h after transfection, although with a reduced amount of total protein with respect to the WT. Concomitantly, almost no p.R510C;p.R561Q was detected at the cell membrane (Fig. 4).

3.5. hCNT1 variants alter protein turnover

Analysis of protein stability was evaluated under different conditions inhibiting protein synthesis, and proteasome or lysosome function. Cells were transfected with WT and variant constructs and after 24 h were treated with cycloheximide to inhibit protein synthesis. Comparison of protein expression after cycloheximide treatment showed a decrease in the half-life of p.R510C, p.R561Q and p.R510C;p.R561Q compared to the WT (Fig. 5A).

Inhibition of the proteasome and lysosome degradation pathways

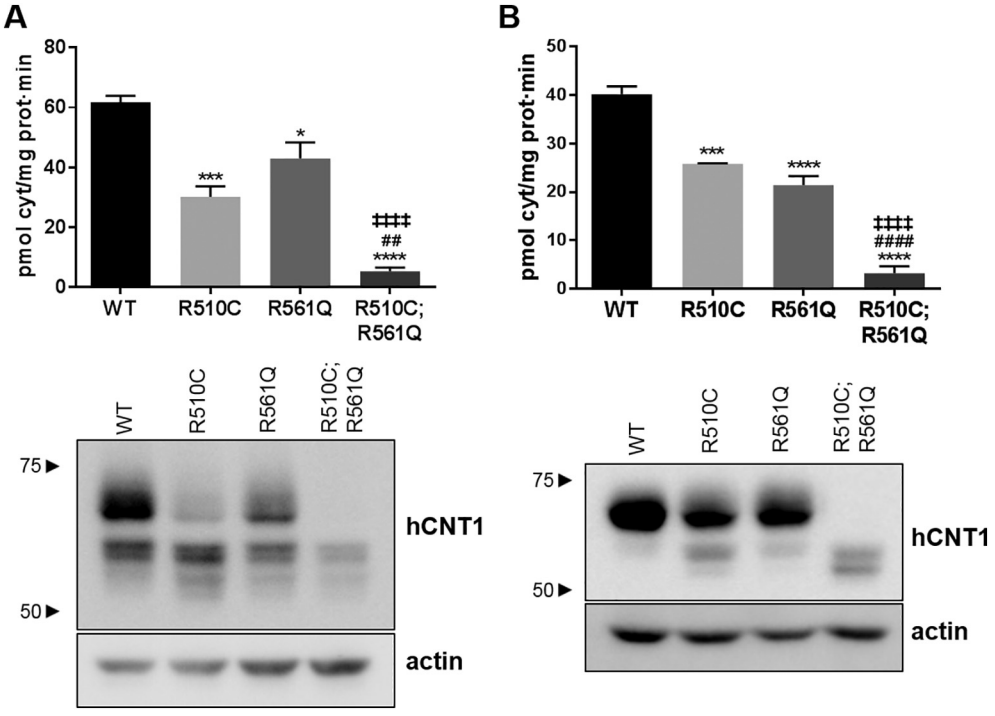

Fig. 3. R510C and R561Q variants modify activity and expression of hCNT1 compared to the WT. HEK293 cells were transfected for either 24 (A) or 48 (B) hours with the different hCNT1 expression vectors, WT, R510C, R561Q and R510C;R561Q. Sodium-dependent transport of [^{3}H]cytidine was calculated as the difference between the cytidine uptake in a NaCl rich medium and in a choline chloride medium. Results were expressed as mean ± SEM ($n = 4$ for 24 h and $n = 3$ for 48 h). The statistical significance was determined by 1 way ANOVA; * indicates the comparison of each variant with the WT, * $p < 0.05$, *** $p < 0.005$, **** $p < 0.0001$; # indicates the comparison of each variant with R510C, ## $p < 0.01$, #### $p < 0.001$; ‡ indicates the comparison between R561Q and R510C;R561Q, ‡‡‡‡ $p < 0.001$. Expression of each hCNT1 protein was analyzed under the same experimental conditions. A representative western blot out of 4 (24 h) and 3 (48 h) independent experiments is shown.

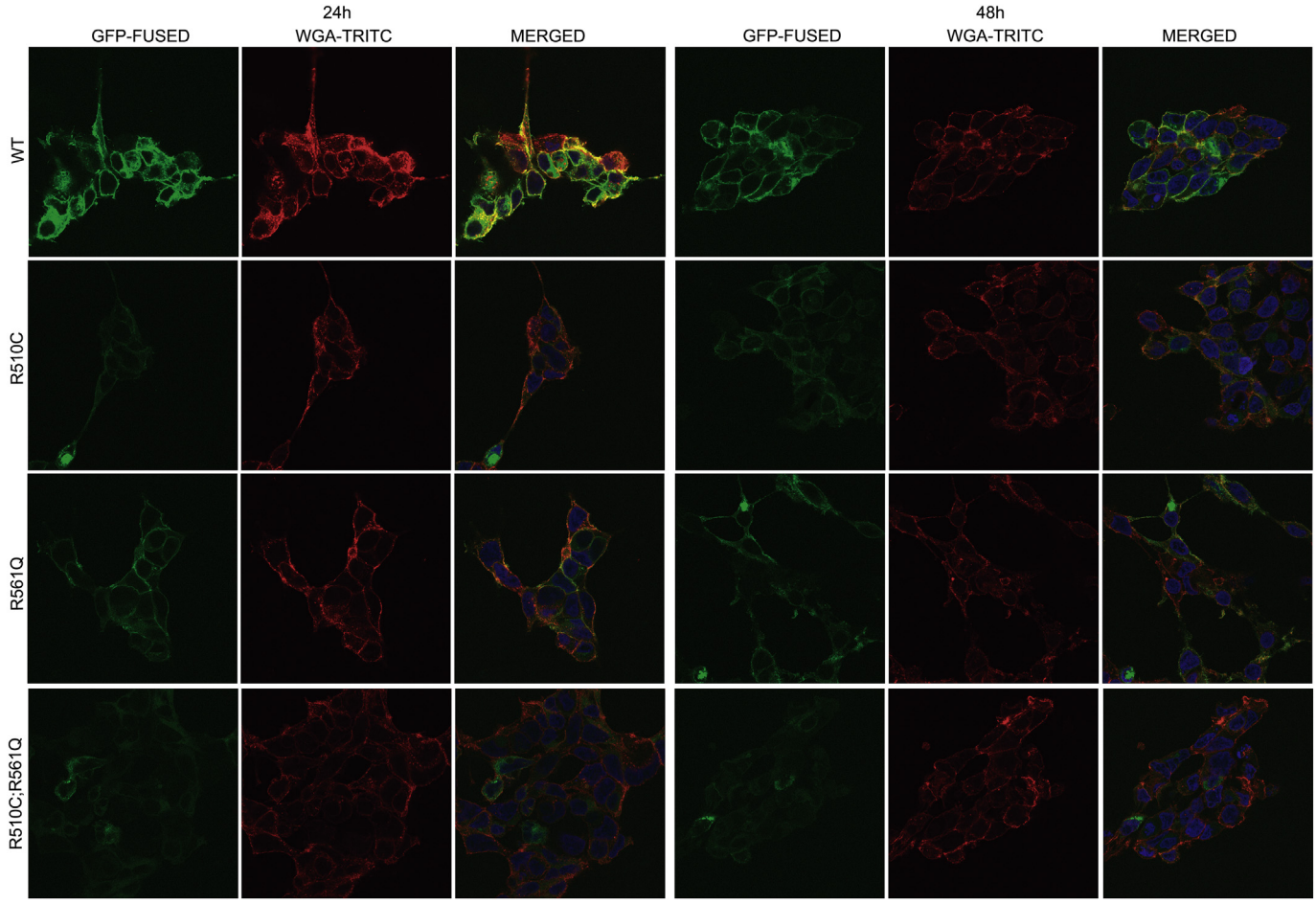

Fig. 4. hCNT1 localization in the plasma membrane is reduced for R510C and R561Q, and imperceptible for R510C;R561Q. Subcellular localization of hCNT1 analyzed by confocal microscopy. GFP-fused hCNT1 vectors were transfected into HEK293 cells for either 24 or 48 h. Cell membrane and nuclei were counterstained with WGA-TRITC and Hoechst, respectively. Magnification ×63.

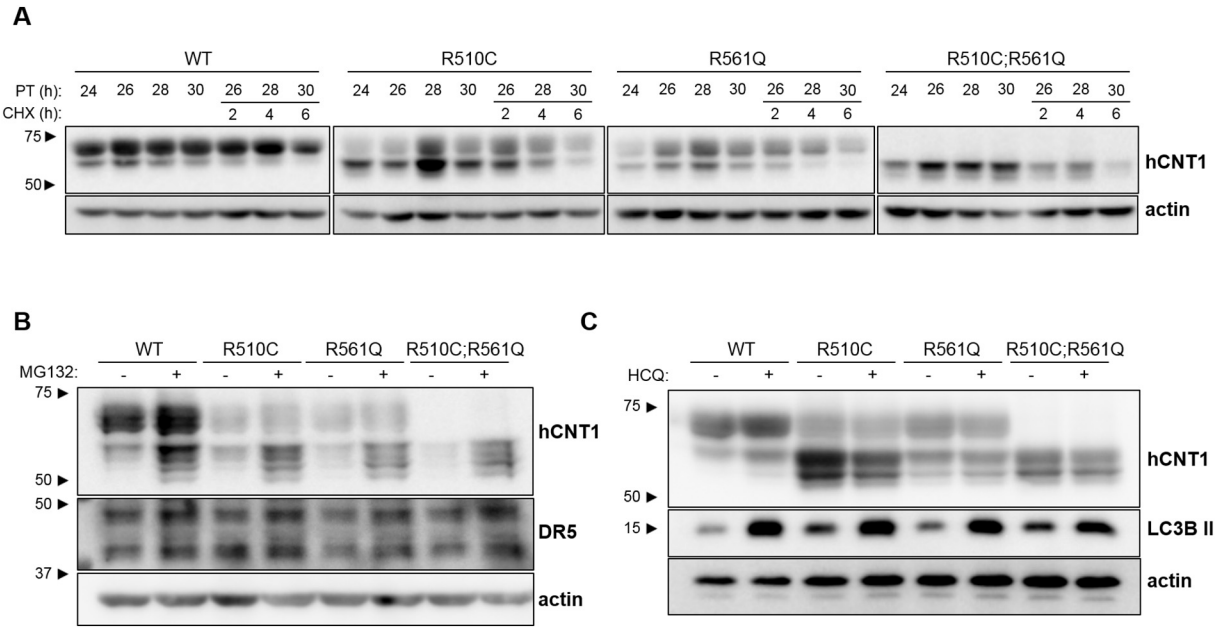

Fig. 5. Protein turnover differs among hCNT1 forms. Western blot analysis of hCNT1 in total cell extracts from transfected HEK293 cells with all the constructs. (A) Cells were treated or not with cycloheximide (CHX, 40 μg/mL) for the indicated time periods after 24 h of transfection. (B) Cells were treated for 16 h at 8 h post-transfection with 5 μM MG-132 or (C) 20 μM hydroxychloroquine sulfate (HCQ). DR5 and LC3B-II were used as positive control, respectively.

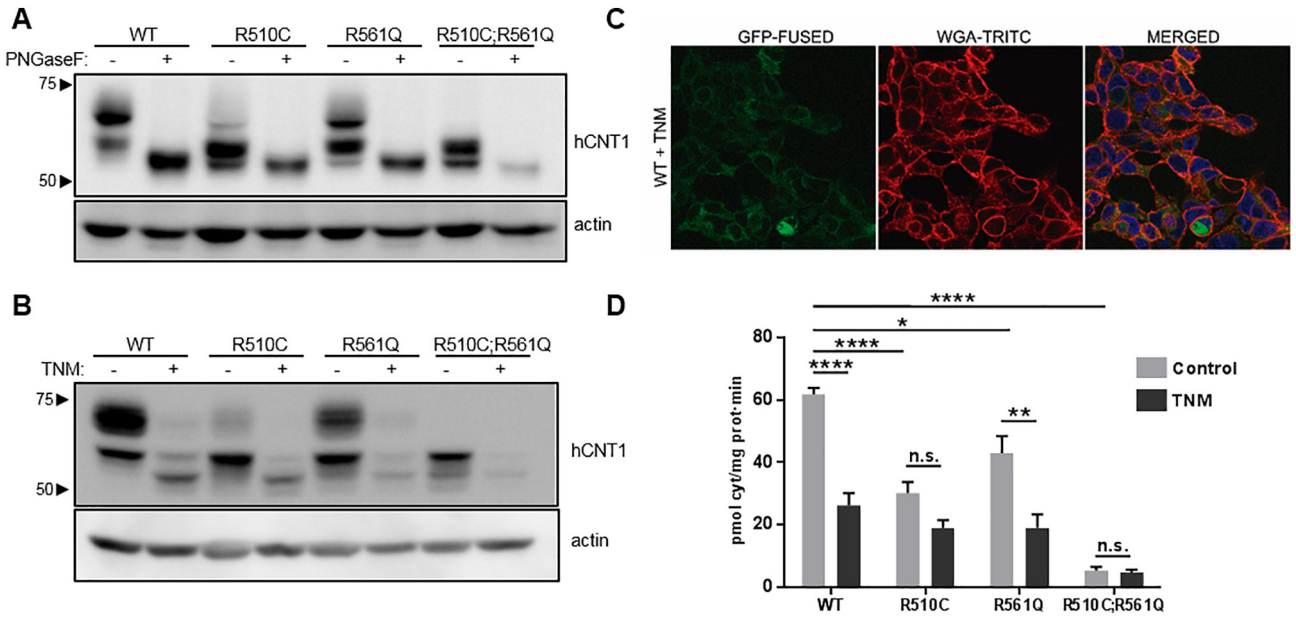

Fig. 6. Glycosylation is determinant for hCNT1 activity. (A) PNGaseF-mediated deglycosylation of N-linked sugars of hCNT1. Cell extracts from transfected HEK293 were treated with PNGaseF for 4 h, and afterwards hCNT1 was detected by western blot. Protein expression (B), localization (C) and activity (D) of HEK293 cells transfected with the different hCNT1 expression vectors, and treated with tunicamycin (TNM, 100 nM) for 16 h. A representative western blot out of 3 independent experiments is shown. hCNT1 sodium-dependent uptake of [^{3}H]cytidine was calculated as the difference between the cytidine uptake in a NaCl medium and in a choline chloride medium. The results were expressed as mean ± SEM (n = 4). The statistical significance was determined by 2 way ANOVA; * $p < 0.05$, ** $p < 0.01$, **** $p < 0.001$.

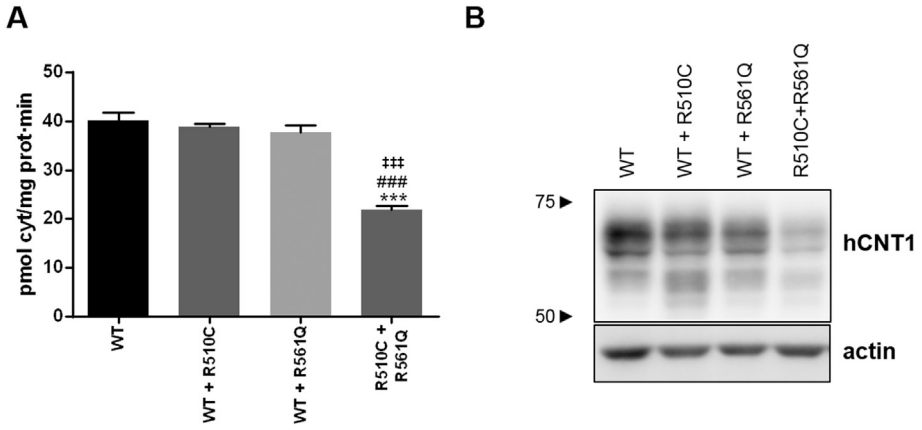

Fig. 7. Allelic disposition of both variants conditions hCNT1 transport activity.
HEK293 cells were cotransfected for 48 h with the different conditions: WT, WT + R510C, WT + R561Q or R510C + R561Q. (A) hCNT1 sodium-dependent uptake of [^{3}H]cytidine, calculated as the difference between the cytidine uptake in a NaCl medium and in a choline chloride medium. The results were expressed as mean ± SEM ($n = 3$). The statistical significance was determined by 1 way ANOVA; * indicates the comparison of each combination with the WT, *** $p < 0.005$; # indicates the comparison of each combination with WT + R510C, ### $p < 0.005$; ‡ indicates the comparison between each combination and WT + R561Q, ‡‡‡ $p < 0.005$. (B) Expression of each hCNT1 protein. A representative western blot out of 3 independent experiments is shown.

was assessed treating the cells with MG132 and hydroxycloroquine, respectively, for 16 h at 8 h post-transfection. An increase in the amount of all constructs was observed after proteasome inhibition, particularly in the low molecular weight bands, whereas no changes were detected after lysosomal pathway inhibition (Fig. 5B,C). These results suggest a key role of proteasome in hCNT1 degradation which is not affected by the different single variants assayed or the combination of both.

3.6. Glycosylation determines hCNT1 transport activity

The different bands observed in hCNT1 WT immunoblot, together with the changes exerted by the different variants alone or combined, prompted us to analyze whether or not hCNT1 is glycosylated. Analysis of hCNT1 putative glycosylation sites by the 'NetNGlyc' predictor identified two possible N-glycosylation residues. Treatment *in vitro* with PNGase F to cleave N-linked glycosylations removed the higher molecular weight bands observed in the western blot against hCNT1 in the WT protein and all the variants (Fig. 6A). To determine the role of hCNT1 glycosylation in transport activity, treatment with the N-glycosylation inhibitor, tunicamycin was performed in cells transfected with all the constructs. Tunicamycin significantly reduced hCNT1 higher molecular weight bands (Fig. 6B) and cell membrane localization (Fig. 6C). Accordingly, WT hCNT1 transport activity was significantly impaired reaching similar levels to p.R510C and p.R561Q after tunicamycin treatment. No changes were observed in the almost undetectable activity of the double mutant (Fig. 6D).

3.7. Heterozygotic trans disposition of p.R510C and p.R561Q aggravates patient phenotype

hCNTs transport function appears to be conditioned by oligomerization [20, 22]. Considering that the patient genetic analysis showed that besides of being heterozygous for both variants, p.R510C and p.R561Q were located in *trans* position, we decided to analyze the effect of putative different heterozygotic combinations. Co-expression of both WT hCNT1 with either p.R510C or p.R561Q had no impact on transport activity. However, in the particular case of this patient, the consequence of in *trans* disposition of both variants, investigated by co-

expression of plasmids carrying p.R510C or p.R561Q, resulted in a significantly impaired transport function (Fig. 7).

3.8. WGS analysis of the patient

To further assess the genome of the patient for additional variants, beyond those identified in *SLC28A1*, we performed singleton whole genome sequencing. We identified 109 candidate genes affected by rare variants: 9 homozygous (*STAMBPL1*, *ABI3BP*, *CELSR2*, *OR5P3*, *MEFV*, *TAF4*, *POU4F1*, *NCOA3* and *ZSWIM6*), 11 hemizygous (*MED12*, *RBMX2*, *GJB1*, *TMLHE*, *WNK3*, *BCOR*, *APLN*, *FAM120C*, *BCOR*, *CXorf30* and *MAGEA4*), and 89 compound heterozygous candidates (*ABCA13*, *ABCC11*, *ABI3BP*, *ADAMTS18*, *ADARB2*, *AGRN*, *AKAP13*, *AMDHD2*, *ANKDD1B*, *ANKZF1*, *ARID4A*, *C15ORF37*, *CCDC92*, *CELSR1*, *CLIC6*, *CORO7*, *CRYBG3*, *D2HGDH*, *DCHS2*, *DLC1*, *DNAH10*, *DNAH11*, *DNAH7*, *DNAH9*, *DPYD*, *EI24*, *ELFN1*, *ELP2*, *ENTHD2*, *ENTPD6*, *FAM47E*, *FAT1*, *FAT3*, *FSTL5*, *GDPD4*, *GIGYF2*, *GPX1*, *GRIK4*, *HERC1*, *HMCN1*, *HOXA4*, *KMT2C*, *KRT24*, *LAMA5*, *LAMB1*, *LGR6*, *LOXL4*, *LRPPRC*, *MMP26*, *MOGAT3*, *MTHFSD*, *MUC12*, *MUC17*, *MUC6*, *MYPN*, *NCOR2*, *NLRP1*, *NRD1*, *OR56B1*, *PCK1*, *PKHD1L1*, *POLQ*, *PRF1*, *PROM1*, *PTX3*, *QRICH2*, *R3HCC1L*, *RLTPR*, *RNF213*, *RNF223*, *RPUSD4*, *SEC24D*, *SELP*, *SLC28A1*, *STRA6*, *SYNE2*, *SYNPO*, *SYVN1*, *TCHHL1*, *TMC3*, *TMPRSS15*, *TMPRSS9*, *TRIM17*, *TTC40*, *TTN*, *USP53*, *WDR38*, *YBX3 and ZNF556*). Beyond the compound heterozygous variants that were previously identified through targeted analysis of *SLC28A1*, the only other candidate gene, among these 109, that fit well with the patient's phenotype of immune dysregulation, fever, hepatosplenomegaly, and liver dysfunction, was the *PRF1* (MIM 170280), which was previously implicated in familial hemophagocytic lymphohistiocytosis type 2 (MIM 603553). The patient was compound heterozygous for a previously described rs147035858 [23] pathogenic frameshift variant: g.72360608CA > C [c.50delT; p.(Leu17Argfs*34); NP_001076585.1]; and a previously described rs745902829 in-frame deletion of g.70598866_70598868del [c.853_855delAAG; p.Lys285del; NP_001076585.1] [24,25]. To determine the mode of inheritance of these variants fragments containing both variants were cloned and Sanger sequenced, confirming that the variants in *PRF1* were in *trans* (Supplemental Fig. 4).

4. Discussion

In this manuscript, we describe the first patient with uridine-cytidineuria likely to be related to a functional deficiency in the pyrimidine nucleoside transporter hCNT1. The two identified variants c.1528C > T (p.R510C) and c.1682G > A (p.R561Q) in *SLC28A1*, encoding hCNT1, altered glycosylation and decreased the half-life of the mutant proteins, resulting in impaired pyrimidine nucleoside transport activity. Taking into account the high prevalence of the c.1528C > T (p.R510C) variant in the East Asian population, it is unlikely that the homozygous c.1528C > T genotype is associated with uridine-cytidineuria or a deleterious clinical phenotype. Further analyses mimicking the genotype of the patient clearly showed that compound heterozygosity, achieved by co-expression of both variants in *trans*, impaired transport activity. In contrast, no changes in hCNT1 activity were observed when both variants were individually co-expressed with the WT hCNT1. These observations suggest that only the expression of the WT form from one allele is sufficient to preserve the activity and it is likely that oligomerization effects might explain these differences in transporter performance. Indeed vcCNT was crystallized as a trimer [20] and hCNT3 is also known to be a trimer *in vivo* [22]. Nevertheless, although the variants examined in this study are likely to affect the monomer structure, it is not evident if they will prevent trimer assembly. The molecular basis for the alteration of hCNT1 glycosylation associated with these genetic variants cannot be elucidated on the basis of our hCNT1 structural model [21] because the putative N-glycosylation sites are located in domains not present in the prokaryotic hCNTs and, therefore, are not present in the homology model recently generated.

The concentration of uridine in plasma, bone marrow and CSF range from approximately 3–8 μM and these levels are tightly regulated by the liver which is the main organ involved in pyrimidine synthesis and degradation [26]. In our patient, normal levels of uridine and only slightly elevated levels of cytidine were observed in plasma, but strongly elevated levels of uridine and cytidine were persistently present in urine. This phenomenon can be explained by the fact that hCNT1 is present in the proximal tubule and glomerulus of the nephron and the apical localization in epithelial cells allows the reabsorption of uridine and cytidine [27].

Uridine and cytidine are essential pyrimidine nucleosides for the brain and the central nervous system and uridine is involved in a number of vital cellular functions, in addition to nucleic acid synthesis [26,28–30]. Uridine behaves as an anticonvulsant in a number of seizure models and uridine competitively inhibited GABA binding to rat cerebellar membranes, frontal cortex, hippocampus and thalamus [26,28]. It is, therefore, conceivable that a hCNT1 deficiency affects intracellular uridine levels and that the altered homeostasis of uridine in the brain is underlying the mild cerebral dysfunction, as indicated by electroencephalographic analysis of our patient.

There is an increased awareness that a combined phenotype of two co-existing monogenic defects resulting in blended phenotypes is an appreciable cause of disease [19]. The rapid deterioration of the patient resulting in multi-organ failure and early death prompted us to investigate whether or not there was another coexisting monogenetic defect in the patient. WGS analysis and subsequent determination of the mode of inheritance demonstrated the presence of two in *trans* pathogenic variants c.50delT; p.(Leu17Argfs*34) and c.853_855del; p.(Lys285del) in the *PRF1* gene. Both variants have previously been identified in patients suffering from Familial Hemophagocytic Lymphohistiocytosis type 2 (FHL-2) [23–25]. FHL-2 is caused by variants of perforin, a toxic pore-forming protein located in cytoplasmic granules that plays a key role in the elimination of viral-infected cells by cytotoxic T-lymphocytes and natural killer cells [16,31,32]. Patients with FHL suffer from fever, (hepato)splenomegaly, bi- or tricytopenia's, hypertriglyceridemia, elevated ferritin, hypofibrinogenemia, hemaphagocytosis, low or absent natural killer cells and markedly elevated lactate dehydrogenase levels [16,31,32]. The excessive cytokine production and immune dysregulation results in tissue damage and ultimately general organ failure. The average survival of patients with FHL, in the absence of treatment, is < 2 months [31]. The clinical presentation of our patient: fever, hepatosplenomegaly, persistent lactic acidosis, severely disturbed liver enzymes and ultimately multi organ failure fits well with the reported phenotype of patients with FHL-2. To our knowledge, it is not known whether other patients with *PRF1* variants, and suffering from FHL-2, presented with uridine-cytidineuria as well.

It is tempting to speculate that the hCNT1 deficiency might have caused the myoclonia and aggravated the clinical demise of our patient. Uridine and cytidine are essential compounds to sustain proliferation of T-lymphocytes and impaired uptake of these pyrimidine nucleosides might have further hampered a proper immune response to a viral infection [33]. It has recently been reported that a proper control of nucleoside intracellular pools in T-cells is a major determinant of T cell survival upon activation and this might explain some phenotypic features of patients lacking lysosomal hENT3 function [13]. In this regard, although hCNT1 mRNA levels in T-cells are almost negligible, they are up-regulated following cell stimulation with phytohemagglutinin (PHA) *ex vivo* [34]. Therefore, an adaptive response of hCNT1 in T-cells could also contribute to modulate nucleoside pools and this function could have been hampered in our patient. In our case, it is conceivable that the presence of two co-existing monogenic defects resulted in a blended clinical and biochemical phenotype. Thus, the clinical presentation of isolated hCNT1 deficiency remains to be established.

Funding

Work at the Pastor-Anglada laboratory has been funded by grant SAF2014-52067-R (Ministerio de Economía y Competitividad, MINECO, Spain), Fundación Ramón Areces and Universitat de Barcelona. This laboratory is a member of CIBER EHD, an initiative of Instituto de Salud Carlos III, Spain. Aida Mata-Ventosa is being funded by a Ph.D. training grant from Formación de Profesorado Universitario (FPU), Ministerio de Educación, Cultura y Deporte (Spain). Work at the Bidon-Chanal laboratory has been funded by grant 2017SGR1746. Work at the Centre for Molecular Medicine and Therapeutics has been funded by the Canadian Institutes of Health Research (grant number #301221); and informatics infrastructure supported by Genome British Columbia and Genome Canada (ABC4DE Project). Clara van Karnebeek is a recipient of the Michael Smith Foundation for Health Research Scholar Award. Britt Drögemöller was funded through the CIHR Postdoctoral Fellowship and the Michael Smith Foundation for Health Research Trainee Award.

Transparency document

The Transparency document associated with this article can be found, in online version.

Acknowledgements

We are grateful to the patient and family for their participation in this study. We acknowledge the clinicians and laboratory scientists involved in the management of this patient, as well as the following individuals for their contributions: Ms. Xiaohua Han for Sanger sequencing; Mrs. Ruth Giesbrecht for administrative support; Ms. Dora Pak and Ms. Evelyn Lomba for research management support; Ms. Michelle Higginson for DNA extraction, sample handling, and technical data; and Ms. Lauren Muttumacoroe for data management.

Conflict of interest statement

The authors declare no conflict of interest.

Appendix A. Supplementary data

Supplementary data to this article can be found online at https://doi.org/10.1016/j.bbadis.2019.01.013.

References

[1] M. Loffler, L.D. Fairbanks, E. Zameitat, A.M. Marinaki, H.A. Simmonds, Pyrimidine pathways in health and disease, Trends Mol. Med. 11 (2005) 430–437.
[2] G.P. Connolly, H.A. Simmonds, J.A. Duley, Pyrimidines and CNS regulation, Trends Pharmacol. Sci. 17 (1996) 106–107.
[3] M. Loffler, E.A. Carrey, E. Zameitat, New perspectives on the roles of pyrimidines in the central nervous system, Nucleosides Nucleotides Nucleic Acids (2018) 1–17.
[4] J.D. Young, S.Y. Yao, J.M. Baldwin, C.E. Cass, S.A. Baldwin, The human concentrative and equilibrative nucleoside transporter families, SLC28 and SLC29, Mol. Asp. Med. 34 (2013) 529–547.
[5] M. Pastor-Anglada, S. Perez-Torras, Emerging roles of nucleoside transporters, Front. Pharmacol. 9 (2018) 606.
[6] S. Balasubramaniam, J.A. Duley, J. Christodoulou, Inborn errors of pyrimidine metabolism: clinical update and therapy, J. Inherit. Metab. Dis. 37 (2014) 687–698.
[7] N. Kamatani, H.A. Jinnah, R.C.M. Hennekam, A.B.P. van Kuilenburg, Purine and Pyrimidine Metabolism, in: D. Rimoin, R. Pyeritz, F.B. Kor (Eds.), Emery & Rimoin's Principles and Practice of Medical Genetics, Elsevier Science Publishing Co Inc., 2013, pp. 1–38.
[8] G. Daniels, B.A. Ballif, V. Helias, C. Saison, S. Grimsley, L. Mannessier, H. Hustinx, E. Lee, J.P. Cartron, T. Peyrard, L. Arnaud, Lack of the nucleoside transporter ENT1 results in the Augustine-null blood type and ectopic mineralization, Blood 125 (2015) 3651–3654.
[9] V. Molho-Pessach, I. Lerer, D. Abeliovich, Z. Agha, A. Abu Libdeh, V. Broshtilova, O. Elpeleg, A. Zlotogorski, The H syndrome is caused by mutations in the nucleoside transporter hENT3, Am. J. Hum. Genet. 83 (2008) 529–534.
[10] S.T. Cliffe, J.M. Kramer, K. Hussain, J.H. Robben, E.K. de Jong, A.P. de Brouwer, E. Nibbeling, E.J. Kamsteeg, M. Wong, J. Prendiville, C. James, R. Padidela, C. Becknell, H. van Bokhoven, P.M. Deen, R.C. Hennekam, R. Lindeman, A. Schenck, T. Roscioli, M.F. Buckley, SLC29A3 gene is mutated in pigmented hypertrichosis with insulin-dependent diabetes mellitus syndrome and interacts with the insulin signaling pathway, Hum. Mol. Genet. 18 (2009) 2257–2265.
[11] N.V. Morgan, M.R. Morris, H. Cangul, D. Gleeson, A. Straatman-Iwanowska, N. Davies, S. Keenan, S. Pasha, F. Rahman, D. Gentle, M.P. Vreeswijk, P. Devilee, M.A. Knowles, S. Ceylaner, R.C. Trembath, C. Dalence, E. Kismet, V. Koseoglu, H.C. Rossbach, P. Gissen, D. Tannahill, E.R. Maher, Mutations in SLC29A3, encoding an equilibrative nucleoside transporter ENT3, cause a familial histiocytosis syndrome (*Faisalabad histiocytosis*) and familial Rosai-Dorfman disease, PLoS Genet. 6 (2010) e1000833.
[12] C.L. Hsu, W. Lin, D. Seshasayee, Y.H. Chen, X. Ding, Z. Lin, E. Suto, Z. Huang, W.P. Lee, H. Park, M. Xu, M. Sun, L. Rangell, J.L. Lutman, S. Ulufatu, E. Stefanich, C. Chalouni, M. Sagolla, L. Diehl, P. Fielder, B. Dean, M. Balazs, F. Martin, Equilibrative nucleoside transporter 3 deficiency perturbs lysosome function and macrophage homeostasis, Science 335 (2012) 89–92.
[13] C.W. Wei, C.Y. Lee, D.J. Lee, C.F. Chu, J.C. Wang, T.C. Wang, W.N. Jane, Z.F. Chang, C.M. Leu, I.L. Dzhagalov, C.L. Hsu, Equilibrative nucleoside transporter 3 regulates T cell homeostasis by coordinating lysosomal function with nucleoside availability, Cell Rep. 23 (2018) 2330–2341.
[14] T. Papinazath, W. Min, S. Sujiththa, A. Cohen, C. Ackerley, C.M. Roifman, E. Grunebaum, Effects of purine nucleoside phosphorylase deficiency on thymocyte development, J. Allergy Clin. Immunol. 128 (2011) 854–863 (e851).
[15] E. Martin, N. Palmic, S. Sanquer, C. Lenoir, F. Hauck, C. Mongellaz, S. Fabrega, P. Nitschke, M.D. Esposti, J. Schwartzentruber, N. Taylor, J. Majewski, N. Jabado, R.F. Wynn, C. Picard, A. Fischer, P.D. Arkwright, S. Latour, CTP synthase 1 deficiency in humans reveals its central role in lymphocyte proliferation, Nature 510 (2014) 288–292.
[16] O. Naneh, T. Avcin, A. Bedina Zavec, Perforin and human diseases, Subcell. Biochem. 80 (2014) 221–239.
[17] H. van Lenthe, A.B.P. van Kuilenburg, T. Ito, A.H. Bootsma, A.G. van Cruchten, Y. Wada, A.H. van Gennip, Defects in pyrimidine degradation identified by HPLC-electrospray tandem mass spectrometry of urine specimens or urine-soaked filter paper strips, Clin. Chem. 46 (2000) 1916–1922.
[18] A.B.P. van Kuilenburg, H. van Lenthe, A.G. van Cruchten, W. Kulik, Quantification of 5,6-dihydrouracil by HPLC-electrospray tandem mass spectrometry, Clin. Chem. 50 (2004) 236–238.
[19] M. Tarailo-Graovac, C. Shyr, C.J. Ross, G.A. Horvath, R. Salvarinova, X.C. Ye, L.H. Zhang, A.P. Bhavsar, J.J. Lee, B.I. Drogemoller, M. Abdelsayed, M. Alfadhel, L. Armstrong, M.R. Baumgartner, P. Burda, M.B. Connolly, J. Cameron, M. Demos, T. Dewan, J. Dionne, A.M. Evans, J.M. Friedman, I. Garber, S. Lewis, J. Ling, R. Mandal, A. Mattman, M. McKinnon, A. Michoulas, D. Metzger, O.A. Ogunbayo, B. Rakic, J. Rozmus, P. Ruben, B. Sayson, S. Santra, K.R. Schultz, K. Selby, P. Shekel, S. Sirrs, C. Skrypnyk, A. Superti-Furga, S.E. Turvey, M.I. Van Allen, D. Wishart, J. Wu, J. Wu, D. Zafeiriou, L. Kluijtmans, R.A. Wevers, P. Eydoux, A.M. Lehman, H. Vallance, S. Stockler-Ipsiroglu, G. Sinclair, W.W. Wasserman, C.D. van Karnebeek, Exome sequencing and the management of neurometabolic disorders, N. Engl. J. Med. 374 (2016) 2246–2255.
[20] Z.L. Johnson, C.G. Cheong, S.Y. Lee, Crystal structure of a concentrative nucleoside transporter from *Vibrio cholerae* at 2.4 A, Nature 483 (2012) 489–493.
[21] C. Arimany-Nardi, A. Claudio-Montero, A. Viel-Oliva, P. Schmidtke, C. Estarellas, X. Barril, A. Bidon-Chanal, M. Pastor-Anglada, Identification and characterization of a secondary sodium-binding site and the main selectivity determinants in the human concentrative nucleoside transporter 3, Mol. Pharm. 14 (2017) 1980–1987.
[22] A. Stecula, A. Schlessinger, K.M. Giacomini, A. Sali, Human concentrative nucleoside transporter 3 (hCNT3, SLC28A3) forms a cyclic homotrimer, Biochemistry 56 (2017) 3475–3483.
[23] S.E. Stepp, R. Dufourcq-Lagelouse, F. Le Deist, S. Bhawan, S. Certain, P.A. Mathew, J.I. Henter, M. Bennett, A. Fischer, G. de Saint Basile, V. Kumar, Perforin gene defects in familial hemophagocytic lymphohistiocytosis, Science 286 (1999) 1957–1959.
[24] K. Goransdotter Ericson, B. Fadeel, S. Nilsson-Ardnor, C. Soderhall, A. Samuelsson, G. Janka, M. Schneider, A. Gurgey, N. Yalman, T. Revesz, R. Egeler, K. Jahnukainen, I. Storm-Mathiesen, A. Haraldsson, J. Poole, G. de Saint Basile, M. Nordenskjold, J. Henter, Spectrum of perforin gene mutations in familial hemophagocytic lymphohistiocytosis, Am. J. Hum. Genet. 68 (2001) 590–597.
[25] U. Zur Stadt, K. Beutel, S. Kolberg, R. Schneppenheim, H. Kabisch, G. Janka, H.C. Hennies, Mutation spectrum in children with primary hemophagocytic lymphohistiocytosis: molecular and functional analyses of PRF1, UNC13D, STX11, and RAB27A, Hum. Mutat. 27 (2006) 62–68.
[26] G.P. Connolly, J.A. Duley, Uridine and its nucleotides: biological actions, therapeutic potentials, Trends Pharmacol. Sci. 20 (1999) 218–225.
[27] S. Rodriguez-Mulero, E. Errasti-Murugarren, J. Ballarin, A. Felipe, A. Doucet, F.J. Casado, M. Pastor-Anglada, Expression of concentrative nucleoside transporters SLC28 (CNT1, CNT2, and CNT3) along the rat nephron: effect of diabetes, Kidney Int. 68 (2005) 665–672.
[28] A. Dobolyi, G. Juhasz, Z. Kovacs, J. Kardos, Uridine function in the central nervous system, Curr. Top. Med. Chem. 11 (2011) 1058–1067.
[29] T. Yamamoto, H. Koyama, M. Kurajoh, T. Shoji, Z. Tsutsumi, Y. Moriwaki, Biochemistry of uridine in plasma, Clin. Chim. Acta 412 (2011) 1712–1724.
[30] M. Cansev, Uridine and cytidine in the brain: their transport and utilization, Brain Res. Rev. 52 (2006) 389–397.
[31] M.R. George, Hemophagocytic lymphohistiocytosis: review of etiologies and management, J. Blood Med. 5 (2014) 69–86.
[32] A. Morimoto, Y. Nakazawa, E. Ishii, Hemophagocytic lymphohistiocytosis:

pathogenesis, diagnosis, and management, Pediatr. Int. 58 (2016) 817–825.
[33] A.A. van den Berg, H. van Lenthe, S. Busch, D. de Korte, A.B. van Kuilenburg, A.H. van Gennip, The roles of uridine-cytidine kinase and CTP synthetase in the synthesis of CTP in malignant human T-lymphocytic cells, Leukemia 8 (1994) 1375–1378.
[34] G. Minuesa, S. Purcet, I. Erkizia, M. Molina-Arcas, M. Bofill, N. Izquierdo-Useros, F.J. Casado, B. Clotet, M. Pastor-Anglada, J. Martinez-Picado, Expression and functionality of anti-human immunodeficiency virus and anticancer drug uptake transporters in immune cells, J. Pharmacol. Exp. Ther. 324 (2008) 558–567.